

КРАТКИЕ СООБЩЕНИЯ

UDC 541.6:547.12:546.17:546.21

4-HYDROXY-2H-1,2-BENZOTIAZINE-3-CARBOHYDRAZIDE 1,1-DIOXIDE-OXALOHYDRAZIDE (1:1):
X-RAY STRUCTURE AND DFT CALCULATIONS

M.N. Arshad¹, O. Şahin², M. Zia-ur-Rehman³, I.U. Khan⁴,
A.M. Asiri¹, H.M. Rafique⁵

¹Department of Chemistry & Center of Excellence for Advanced Materials Research (CEAMR) Faculty of Science, King Abdulaziz University, Jeddah, Saudi Arabia

²Scientific and Technological Research Application and Research Center, Sinop University, Sinop, Turkey
E-mail: onurs@omu.edu.tr

³Applied Chemistry Research Center, PCSIR, Laboratories Complex Ferozpur Road, Lahore, Pakistan

⁴Materials Chemistry Laboratory, Department of Chemistry, GC University, Lahore, Pakistan

⁵X-ray Diffraction and Crystallography Laboratory, Department of Physics, School of Physical Sciences, University of the Punjab, Lahore, Pakistan

Received November, 18, 2011

Revised — June, 2, 2012

The title compound, 4-hydroxy-2H-1,2-benzothiazine-3-carbohydrazide 1,1-dioxide-oxalo-hydrazide (1:1), is determined using X-ray diffraction techniques and the molecular structure is also optimized at the B3LYP/6-31G(*d,p*) level using density functional theory (DFT). The asymmetric unit consists of four independent molecules. The oxalo-hydrazide molecules have the centre of symmetry at the mid-point of the central C—C bond. Each thiazine ring adopts a *half-chair* conformation. Intermolecular C—H...O, N—H...O and N—H...N hydrogen bonds produce *R*₂²(10), *R*₂²(13), *R*₃³(12) and *R*₃³(15) rings, which lead to one-dimensional polymeric chains. An extensive three-dimensional supramolecular network of N—H...N, N—H...O, C—H...O and O—H...O hydrogen bonds is responsible for crystal structure stabilization.

Keywords: X-ray diffraction analysis, benzothiazine, oxalo-hydrazide, DFT, Mulliken atomic charge, molecular electrostatic potential.

Synthesis and structural characterization of carbohydrazides and their derivatives is much focused in the recent literature due to their applications in biochemistry as well as in materials synthesis *via* complexation [1, 2]. They are well known for their anti-viral [3], anti-tuberculosis [4], anti-fungal [5], bacteriostatic [6], insecticidal [7] and anti-parasitic [8] activities. As part of a research program regarding the synthesis of new derivatives of benzothiazine 1,1-dioxides [9, 10], the synthesis and crystal structure of 4-hydroxy-2H-1,2-benzothiazine-3-carbohydrazide 1,1-dioxide-oxalo-hydrazide (1:1) is reported here.

The title compound was synthesized from commercially available saccharin, which was converted to methyl 4-hydroxy-2H-1,2-benzothiazine-3-carboxylate 1,1-dioxide by a reported procedure [11] and was subsequently subjected to hydrazinolysis in methanol along with equimolar dimethyl oxalate. It was interesting to note that dimethyl oxalate did not react with benzothiazine hydrazide under these reaction conditions, but reacted with hydrazine and co-crystallized with the product oxalo-hydrazide.

Experimental. Synthesis. A mixture of methyl 4-hydroxy-2H-1,2-benzothiazine-3-carboxylate 1,1-dioxide (2.00 g, 7.84 mmol), hydrazine hydrate (1.57 g, 31.36 mmol) and dimethyl oxalate (1.02 g, 39.2 mmol) was stirred in ethanol (30 ml) for half an hour. On completion of reaction, as indi-

Table 1

Crystal and refinement data for **1**

Molecular formula	C ₂₀ H ₂₄ N ₁₀ O ₁₀ S ₂
Molecular mass	628.61
Crystal system	Triclinic
Space group	P-1
Unit cell parameters <i>a</i> , <i>b</i> , <i>c</i> , Å	5.6319(8), 14.380(2), 16.035(2)
α , β , γ , deg.	103.124(2), 90.457(3), 90.828(3)
<i>V</i> , Å ³	1264.5(3)
<i>Z</i>	2
ρ_{calc} , g/cm ³	1.651
<i>T</i> , K	173
Radiation; λ , Å	MoK _α ; 0.71073
Crystal size, mm	0.46×0.13×0.09
Color	White
Crystal shape	Block
Reflections measured	11183
$\theta_{\min,\max}$, deg.	2.7—28.3
Independent reflections	6330 [$R_{\text{int}} = 0.021$]
Parameters refined	427
Final <i>R</i> factor [$I > 2\sigma(I)$]	$R_1 = 0.035$, $wR_2 = 0.092$
<i>R</i> factor (all data)	$R_1 = 0.046$, $wR_2 = 0.084$
GOOF	1.01
Residual electron density (min/max), e/Å ³	-0.40/0.44

cated by TLC (thin layer chromatography), solvent was removed under vacuum. Solid residue obtained was crystallized in methanol to get hygroscopic crystals.

X-ray diffraction analysis. X-ray diffraction data were collected at 173 K on a Siemens SMART three-circle X-ray diffractometer equipped with an APEX II CCD detector (Bruker-AXS) and an Oxford cryosystems 700 cryostream, using MoK_α radiation (0.71073 Å) and a graphite monochromator and the data were corrected for Lorentz and polarization effects and for absorption using the multi-scan method [12, 13]. The structures were solved by direct methods using SHELXS-97 and refined by full-matrix least-squares methods on F^2 using SHELXL-97 [14] from within the WINGX [15] suite of software. All non-hydrogen atoms were refined anisotropically. All H atoms bound to C atoms were refined using a riding model, with C—H = 0.93 Å and $U_{\text{iso}}(\text{H}) = 1.2U_{\text{eq}}(\text{C})$ for aromatic C atoms. All other H atoms bound to N and O atoms were located in difference maps and refined freely. Supramolecular analyses were made and the diagrams were prepared with the aid of PLATON [16]. Crystal data and parameters of the structural experiment are given in Table 1. Atomic coordinates have been deposited to the Cambridge Structural Database (<http://www.ccdc.cam.ac.uk>): CCDC 805426. The hydrogen bonds are characterized in Table 3.

Computational procedure. The geometry optimization of the molecule leading to energy minima was achieved using the B3LYP hybrid exchange-correlation functional with the 6-31G(*d,p*) basis set [17, 18]. The calculations were started from the crystallographically achieved geometries of the molecule. All calculations in this work were carried out using the GAUSSIAN03W package [19]. The optimized molecular geometry, total molecular energy and dipole moment calculations were obtained from the computational process.

Results and discussion. Crystal structure. The molecular structure and atom-labeling scheme are shown in Fig. 1. The asymmetric unit of **1** consists of two oxalohydrazide molecules and two C₉H₉N₃O₄S molecules. The oxalohydrazide molecules have the centre of symmetry at the mid-point of

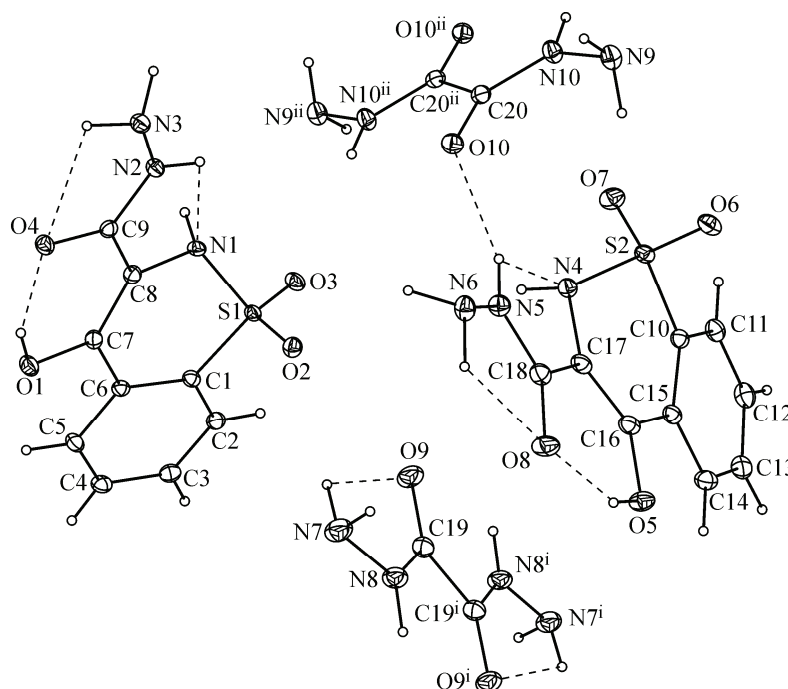


Fig. 1. View of the molecule of **1**, showing the atom numbering scheme. Displacement ellipsoids are drawn at the 30% probability. Intramolecular hydrogen bonds are indicated by dashed lines

the central C—C [C(19)—C(19)ⁱ and C(20)—C(20)ⁱⁱ] bond. The bond distances of S=O ranged between 1.4320(11) Å and 1.4398(12) Å. These bond lengths are within normal ranges [20, 21]. The bond distances of C=O ranged between 1.2351(18) Å and 1.2630(18) Å. The N(7)—N(8)—C(19)—O(9) and N(9)—N(10)—C(20)—O(10) torsion angles are 3.3(3)° and 1.0(3)°. The bond angles and torsion angles of oxalohydrazide molecules are similar to that in abundant polymorphism in a system with multiple hydrogen-bonding opportunities: oxalyl dihydrazide [22]. The selected bond lengths and angles are given in Table 2. The heterocyclic thiazine ring [N(1)/C(8)/C(7)/C(6)/C(1)/S(1)] adopts a *half-chair* conformation wherein N(1) is displaced by 0.2931(9) Å (N(4) is displaced by 0.2782(9) Å) from the plane defined by the remaining atoms in the ring, with puckering parameters [23]:

Table 2

Comparison of the optimized and experimental geometric parameters of **1** (Å and deg.)

Bond	X-ray	DFT	Bond	X-ray	DFT	Bond Angles	X-ray	DFT
C(1)—S(1)	1.7580(16)	1.7899	O(2)—S(1)	1.4333(12)	1.4590	O(2)—S(1)—O(3)	118.69(7)	121.611
C(10)—S(2)	1.7586(17)		O(7)—S(2)	1.4320(11)		O(7)—S(2)—O(6)	117.92(7)	
O(3)—S(1)	1.4351(11)	1.4626	N(1)—S(1)	1.6165(13)	1.6967	N(1)—S(1)—C(1)	103.67(7)	100.366
O(6)—S(2)	1.4398(12)		N(4)—S(2)	1.6211(13)		N(4)—S(2)—C(10)	103.50(7)	
C(19)—O(9)	1.2362(19)	1.2353	C(9)—O(4)	1.2630(18)	1.2609	O(2)—S(1)—N(1)	108.74(7)	108.016
C(20)—O(10)	1.2351(18)		C(18)—O(8)	1.2606(18)		O(6)—S(2)—N(4)	108.96(7)	
N(2)—N(3)	1.4161 (19)	1.4060	C(7)—O(1)	1.3456(18)	1.3320	O(3)—S(1)—N(1)	107.71(7)	106.422
N(5)—N(6)	1.4213 (19)		C(16)—O(5)	1.3448(18)		O(7)—S(2)—N(4)	107.49(7)	
N(7)—N(8)	1.412 (2)	1.4055				O(3)—S(1)—C(1)	109.45(7)	109.299
N(9)—N(10)	1.4159 (18)					O(6)—S(2)—C(10)	107.57(7)	
						O(2)—S(1)—C(1)	107.56(7)	109.006
						O(7)—S(2)—C(10)	110.44(7)	

Table 3

Parameters of hydrogen bonds for **1** (\AA and deg.)

D—H...A	<i>d</i> (D—H)	<i>D</i> (H...A)	\angle DHA	<i>d</i> (D...A)	Symmetry operations
N(5)—H(5A)...O(10)	0.83(2)	2.11(2)	2.9018(18)	159.8(19)	<i>x, y, z</i>
O(1)—H(1A)...O(4)	0.83(2)	1.79(2)	2.5665(17)	154(2)	<i>x, y, z</i>
O(5)—H(5B)...O(8)	0.90(2)	1.76(2)	2.5630(17)	147.8(19)	<i>x, y, z</i>
C(11)—H(11)...O(6)	0.93	2.53	3.178(2)	127	<i>x+1, y, z</i>
N(4)—H(4A)...N(6)	0.88(2)	1.98(2)	2.832(2)	163.7(19)	<i>x+1, y, z</i>
N(1)—H(1)...N(3)	0.938(19)	1.910(19)	2.8410(19)	171.1(17)	<i>x+1, y, z</i>
N(10)—H(10)...O(3)	0.87(2)	2.05(2)	2.8489(17)	152.3(18)	$-x+1, -y+1, -z+1$
N(3)—H(3B)...O(6)	0.89(2)	2.20(2)	3.0776(18)	168.3(17)	$-x, -y+1, -z+1$
N(2)—H(2A)...N(9)	0.82(2)	2.17(2)	2.9296(19)	154.7(19)	$-x, -y+1, -z+1$
N(8)—H(8)...O(8)	0.86(2)	1.96(2)	2.7526(18)	152(2)	$-x-1, -y+1, -z$
N(3)—H(3A)...O(4)	0.87(2)	2.16(2)	2.8771(17)	139.5(17)	$-x, -y+2, -z+1$
N(9)—H(9A)...O(7)	0.88(2)	2.32(2)	2.8564(18)	119.9(17)	$x-1, y, z$
N(7)—H(7A)...O(2)	0.86(2)	2.31(2)	2.9946(19)	136.0(19)	$x-1, y, z$
N(6)—H(6A)...O(9)	0.88(2)	2.31(2)	3.1144(18)	151.5(18)	$x-1, y, z$
N(6)—H(6B)...O(2)	0.87(2)	2.37(2)	2.9919(18)	129.1(17)	$x-1, y, z$
N(6)—H(6B)...O(3)	0.87(2)	2.51(2)	3.0843(18)	124.3(16)	$x-2, y, z$
N(9)—H(9B)...O(10)	0.89(2)	2.21(2)	3.0882(19)	168.5(18)	$-x-1, -y+1, -z+1$

$Q = 0.4468(12) \text{ \AA}$, $\theta = 62.03(19)^\circ$ and $\phi = 28.9(2)^\circ$ ($Q = 0.4292(12) \text{ \AA}$, $\theta = 118.7(2)^\circ$ and $\phi = 26.8(2)^\circ$ in N(4)/C(17)/C(16)/C(15)/C(10)/S(2) ring). Least-squares mean plane calculations of phenyl ring (C(1)~C(6) and C(10)~C(15)) planes show that these are approximately planar, with respective maximum deviations of 0.0079(10) \AA for C(1) and 0.0128(11) \AA for C(15). The dihedral angles between thiazine and phenyl ring planes are 9.44(9) $^\circ$ and 9.98(8) $^\circ$.

The molecules of **1** are linked by intermolecular hydrogen bonding, and we employ graph-set notation [24] to describe the patterns of hydrogen bonding. Molecules of **1** are linked into sheets by a combination of N—H...N, N—H...O, C—H...O and O—H...O hydrogen bonds (Table 3). Within the selected asymmetric unit, intramolecular O—H...O, N—H...N and N—H...O hydrogen bonds produce S(5)S(6) motifs. The C(11) atom in the molecule at (x, y, z) acts as hydrogen-bond donor, via H(11), to the O(6)ⁱⁱⁱ atom, so forming a C(5) chain running parallel to the [100] direction. The N(4) atom in the molecule at (x, y, z) acts as hydrogen-bond donor, via H(4A), to the N(6)ⁱⁱⁱ atom, so forming a C(6) chain running parallel to the [100] direction. The combination of C(5) and C(6) chains generates a chain of edge-fused $R_2^2(13)$ rings running parallel to the [100] direction. Similarly, the N(1) atom in the molecule at (x, y, z) acts as hydrogen-bond donor, via H(1), to the N(3)ⁱⁱⁱ atom, so forming a C(6) chain running parallel to the [100] direction (Fig. 2). The combination of N(3)—H(3B)...O(6)ⁱⁱ, N(2)—H(2A)...N(9)ⁱⁱ and N(5)—H(5A)...O(10)

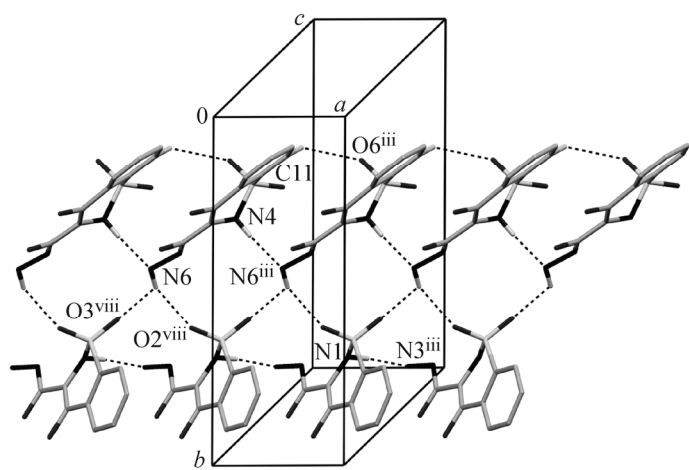


Fig. 2. Part of the crystal structure of **1**, showing the formation of a chain generated by the C—H...O, N—H...N and N—H...O hydrogen bonds (dashed lines; Table 3)

generates a chain of edge-fused $R_2^2(13)$ rings running parallel to the [100] direction. Similarly, the N(1) atom in the molecule at (x, y, z) acts as hydrogen-bond donor, via H(1), to the N(3)ⁱⁱⁱ atom, so forming a C(6) chain running parallel to the [100] direction (Fig. 2). The combination of N(3)—H(3B)...O(6)ⁱⁱ, N(2)—H(2A)...N(9)ⁱⁱ and N(5)—H(5A)...O(10)

Table 4

Mulliken atomic charges for compound 1

C(1)	-0.239980	C(6)	0.114758	C(11)	0.549187	N(5)	-0.378047	O(3)	-0.514853
C(2)	-0.042333	C(7)	0.280568	N(1)	-0.670441	N(6)	-0.385751	O(4)	-0.616858
C(3)	-0.030406	C(8)	0.088101	N(2)	-0.386691	N(7)	-0.374925	O(5)	-0.546866
C(4)	-0.048344	C(9)	0.632951	N(3)	-0.375645	O(1)	-0.458888	O(6)	-0.559926
C(5)	-0.035177	C(10)	0.549303	N(4)	-0.385669	O(2)	-0.477576	S(1)	1.142136

hydrogen bonds generates a $R_3^3(15)$ ring. The N(3) amino atom in the molecule at (x, y, z) acts as hydrogen-bond donor, via H(3A), to the O(4)^{vi} atom, so forming a centrosymmetric $R_2^2(10)$ ring centered at $(0, 1, 1/2)$. The combination of N(9)—H(9A)...O(7)^{vii}, N(5)—H(5A)...O(10) and N(4)—H(4A)...N(6)ⁱⁱⁱ hydrogen bonds generates a $R_3^3(12)$ ring. The N(9) amino atom in the molecule at (x, y, z) acts as hydrogen-bond donor, via H(9B), to the O(10)^{ix} atom, so forming a centrosymmetric $R_2^2(10)$ ring centered at $(1/2, 1/2, 1/2)$.

Energetics, dipole moments and Mulliken charges. As seen from Table 2, the optimized bond lengths are slightly different from the experimental values. The biggest difference of the bond lengths between the experimental and predicted values are found at N(1)—S(1) and N(4)—S(2) bonds, with the different values being 0.080 Å and 0.076 Å for the B3LYP method. For the bond angles, the biggest differences are observed for O(2)—S(1)—O(3) and O(6)—S(2)—O(7); the different values are 2.921° and 3.691°. According to the above comparisons, it can be deduced that, for the title compound, the biggest differences of the bond lengths and bond angles are mainly found in the groups involved in the hydrogen bonds, which can be easily understood taking into account the intermolecular hydrogen bond interactions present in the crystal. In the DFT/B3LYP calculations, the total energy of the optimized geometry and the dipole moment are obtained as -7.242×10^{-15} J and 3.9727 D for 1. Mulliken charges were calculated by determining the electron population of each atom as defined by the basis sets. According to the calculated results for Mulliken atomic charge analysis, oxygen and nitrogen atoms, as expected, have larger negative charges relative to other atoms (Table 4).

Frontier molecular orbitals and the molecular electrostatic potential. Fig. 3 shows the distributions and energy levels of the HOMO-1, HOMO, LUMO and LUMO +1 orbitals computed at the DFT/B3LYP/6-31G(*d,p*) level for the title compound. Both the highest occupied molecular orbitals (HOMOs) and the lowest unoccupied molecular orbitals (LUMOs) are mainly localized on the rings, indicating that the HOMO-LUMO are mostly the π -antibonding type orbitals. As can be seen in Fig. 4, there are several possible sites of electrophilic attack (red regions). The negative V(r) values of 1 are

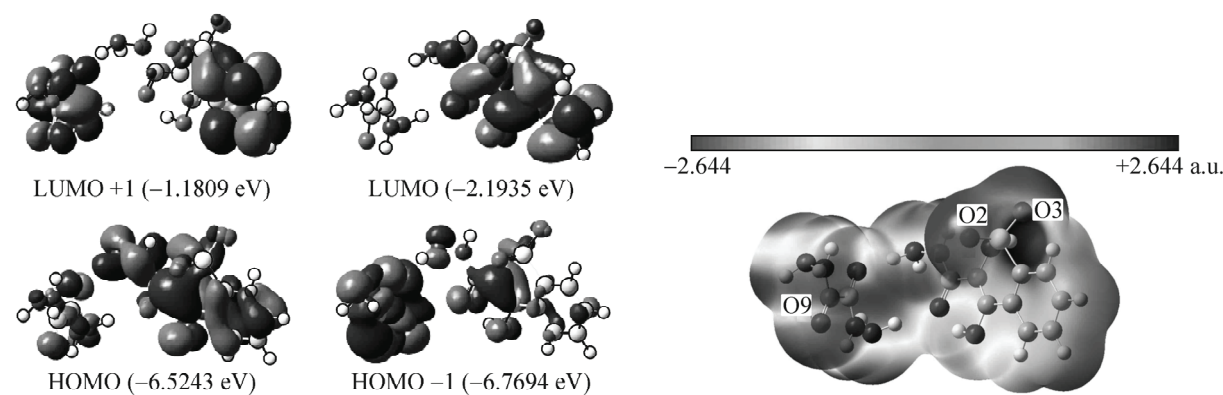


Fig. 3. Molecular orbital surfaces and energy levels given in parentheses for the LUMO+1, LUMO, HOMO and HOMO-1 of 1 computed at the DFT/B3LYP/6-31G(*d,p*) level

Fig. 4. Molecular electrostatic potential map of 1 calculated at the DFT/B3LYP/6-31G(*d,p*) level

–0.047 a.u. for O(2) atom, which is the most negative region; about –0.043 and –0.041 a.u. for O(3) and O(9) atoms, which are the least negative region. However, the maximum positive regions are localized on the hydrogen atoms, which can be considered as possible sites for nucleophilic attack (blue regions), with the maximum value of 0.053 a.u. According to these calculated results, the MEP map shows that the negative potential sites are on the electronegative atoms and the positive potential sites are around the hydrogen atoms.

Acknowledgements. M.N. Arshad acknowledges Higher Education Commission of Pakistan for providing scholarship under IRSIP scheme (PIN # IRSIP-10-ps-02) and also K Travis Holman Department of Chemistry, Georgetown University, Washington, DC, USA for providing lab facility.

REFERENCES

1. Huang Z., Liu Y., Li Y., Xiong L., Cui Z., Song H., Liu H., Zhao Q., Wang Q. // J. Agric. Food Chem. – 2011. – **59**(2). – P. 635.
2. El-Asmy A.A., El-Gammal O.A., Radwan H.A. // Spectrochim. Acta Part A. – 2010. – **76**. – P. 496.
3. Ochiai T., Ishida R. // Jpn. J. Pharmacol. – 1982. – **32**. – P. 427.
4. Lopez S.E., Rosales M.E., Canelon C.E., Valverode E.A., Narvaez R.C., Charris J.E., Giannini F.A., Enriz R.D., Carrasco M., Zacchino S. // Hetrocycl. Commun. – 2000. – 7. – P. 473.
5. Tani J., Yamada Y., Oine T., Ochiai T., Ishida R., Inoue I. // J. Med. Chem. – 1979. – **22**. – P. 95.
6. Raffa D., Daidone G., Schillaci D., Maggio B., Plescia F. // Pharmazie. – 1999. – **54**. – P. 251.
7. Farqhaly A.O., Moharram A.M. // Boll. Chim. Farm. – 1999. – **138**. – P. 280.
8. Jantova S., Greif G., Spirkova K., Stankovsky S., Oravcova M. // Folia Microbiol. (Praha). – 2000. – **45**. – P. 133.
9. Zia-ur-Rehman A., Choudary J.A., Elsegood M.R.J., Siddiqui H.L., Khan K.M. // Eur. J. Med. Chem. – 2009. – **44**. – P. 1311.
10. Ahmed M., Siddiqui H.L., Zia-ur-Rehman M., Parvez M. // Eur. J. Med. Chem. – 2010. – **45**. – P. 698.
11. Lombardino J.G., Wiseman E.H., McLamore W.M. // J. Med. Chem. – 1971. – **14**. – P. 1171.
12. Otwinowski Z., Minor W. // Methods Enzymol. – 1997. – **276**. – P. 307.
13. Hooft R. COLLECT. Nonius BV, Delft, The Netherlands, 1998.
14. Sheldrick G.M. // Acta Crystallogr. – 2008. – **A64**. – P. 112.
15. Farrugia L.J.J. // Appl. Crystallogr. – 1999. – **32**. – P. 837.
16. Spek A.L. // J. Appl. Crystallogr. – 2003. – **36**. – P. 7.
17. Lee C., Yang W., Parr R.G. // Phys. Rev. B. – 1988. – **37**. – P. 785.
18. Becke A.D. // J. Chem. Phys. – 1993. – **98**. – P. 5648.
19. Frisch M.J., Trucks G.W., Schlegel H.B., Scuseria G.E., Robb M.A., Cheeseman J.R., Montgomery J.A. Jr., Vreven T., Kudin K.N., Burant J.C., Millam J.M., Iyengar S.S., Tomasi J., Barone V., Mennucci B., Cossi M., Scalmani G., Rega N., Petersson G.A., Nakatsuji H., Hada M., Ehara M., Toyota K., Fukuda R., Hasegawa J., Ishida M., Nakajima T., Honda Y., Kitao O., Nakai H., Klene M., Li X., Knox J.E., Hratchian H.P., Cross J.B., Bakken V., Adamo C., Jaramillo J., Gomperts R., Stratmann R.E., Yazyev O., Austin A.J., Cammi R., Pomelli C., Ochterski J.W., Ayala P.Y., Morokuma K., Voth G.A., Salvador P., Dannenberg J.J., Zakrzewski V.G., Dapprich S., Daniels A.D., Strain M.C., Farkas O., Malick D.K., Rabuck A.D., Raghavachari K., Foresman J.B., Ortiz J.V., Cui Q., Baboul A.G., Clifford S., Cioslowski J., Stefanov B.B., Liu G., Liashenko A., Piskorz P., Komaromi I., Martin R.L., Fox D.J., Keith T., Al-Laham M.A., Peng C.Y., Nanayakkara A., Challacombe M., Gill P.M.W., Johnson B., Chen W., Wong M.W., Gonzalez C., Pople J.A. Gaussian 03, Revision E. 01, Gaussian, Inc. Pittsburgh, PA 2003.
20. Arshad M.N., Tahir M.N., Khan I.U., Shafiq M., Siddiqui W.A. // Acta Crystallogr. – 2008. – **E64**. – P. o2045.
21. Siddiqui W.A., Ahmad S., Siddiqui H.L., Tariq M.A., Parvez M. // Acta Crystallogr. – 2007. – **E63**. – P. o4585.
22. Ahn S., Guo F., Kariuki B.M., Harris K.D.M. // J. Amer. Chem. Soc. – 2006. – **128**. – P. 8441.
23. Cremer D., Pople J.A. // J. Amer. Chem. Soc. – 1975. – **97**. – P. 1354.
24. Bernstein J., Davis R.E., Shimoni L., Chang N.-L. // Angew Chem Int Ed Engl. – 1995. – **34**. – P. 1555.